A family of mononuclear Co^{III}/2-pyridyloximate complexes and their conversion to trinuclear, mixed-valence linear Co$^{II/III}_3$ clusters

Theocharis C. Stamatatos [a,b], Eugenia Katsoulakou [a], Aris Terzis [c], Catherine P. Raptopoulou [c], Richard E.P. Winpenny [b,*], Spyros P. Perlepes [a,*]

[a] Department of Chemistry, University of Patras, 265 04 Patras, Greece
[b] School of Chemistry, The University of Manchester, Oxford Road, Manchester M13 9PL, UK
[c] Institute of Materials Science, NCSR "Demokritos", 153 10 Aghia Paraskevi Attikis, Greece

ARTICLE INFO

ABSTRACT

The use of the 2-pyridyl oxime ligands (LH) 2-pyridinealdoxime, methyl 2-pyridyl ketone oxime and phenyl 2-pyridyl ketone oxime in Co chemistry has been investigated and led to two families of compounds. The first family includes the mononuclear octahedral, low-spin complexes [Co^{III}(L)$_3$], while the second family consists of the trinuclear, mixed-valent linear clusters [Co$^{III}_2$Co^{II}(L)$_6$]X$_2$ (X = ClO$_4^-$, PF$_6^-$). The latter are prepared by the reactions of the former with an appropriate Co^{II} source. The structural, physical and spectroscopic properties of the complexes are described.

1. Introduction

The cluster chemistry of 3d metals at intermediate oxidation states has been attracting intense interest during the last several years [1]. This is due to the combination of the aesthetically pleasing structures that many such molecular clusters possess and the often unusual and even novel magnetic properties that some of them display. In particular, some of these clusters have been found to be single-molecule magnets (SMMs), which are individual molecules capable of functioning as nanoscale magnetic particles and which thus represent a molecular approach to nanomagnetism [2]. The magnetic behaviour of SMMs results from the combination of a large ground spin state (S) with a large and negative Ising (or easy-axis) type of magnetoanisotropy, as measured by the axial zero-field splitting parameter D [2]. Most of the known SMMs are Mn clusters containing at least some Mn^{III} centers. Cobalt(II), which has a large single-ion anisotropy due to the orbitally degenerate ground state, may be a good candidate for making SMMs, and few polynuclear Co(II) complexes that show SMM properties have been reported [3].

The present results were obtained as part of our continuing efforts in Co cluster chemistry [4] and have now led to mixed-valent Co$_2^{III}$Co^{II} complexes, which were prepared by using both the "metal complexes as ligands" strategy [5] and "one-pot" procedures. The ligands used in our efforts are the 2-pyridinealdoxime (paoH), methyl 2-pyridyl ketone oxime (mpkoH) and phenyl 2-pyridyl ketone oxime (ppkoH), see Scheme 1. These ligands belong to the family of 2-pyridyl oximes [6] and their anionic forms have been used to prepare SMMs [7] and single-chain magnets [8].

We herein describe the syntheses, crystal structures and physical characterization of Co$^{III}_2$Co^{II} clusters and their mononuclear Co^{III} precursors, all featuring the deprotonated ligands pao$^-$, mpko$^-$ and ppko$^-$. Portions of this work have been previously communicated [9].

2. Experimental

2.1. General and physical measurements

All manipulations were performed under aerobic conditions using materials (reagent grade) and solvents as received. mpkoH was prepared as described elsewhere [10]. WARNING: Perchlorate salts are potentially explosive; such compounds should be synthesized and used in small quantities, and treated with utmost care at all times.

Microanalyses (C, H, N) were performed by the University of Ioannina (Greece) Microanalytical Laboratory using an EA 1108 Carlo Erba analyser. IR spectra (4000–450 cm^{-1}) were recorded on Perkin–Elmer 16 PC and Nicolet 520 FTIR spectrometers with samples prepared as KBr pellets. Solid-state (diffuse reflectance, 28.5–12.5 kK) electronic spectra were recorded on a Varian Cary

* Corresponding authors. Tel.: +30 2610 997146; fax: +30 2610 997118.
E-mail addresses: richard.winpenny@man.ac.uk (R.E.P. Winpenny), perlepes@patras.upatras.gr (S.P. Perlepes).

R=H; paoH

R=Me; mpkoH

R=Ph; ppkoH
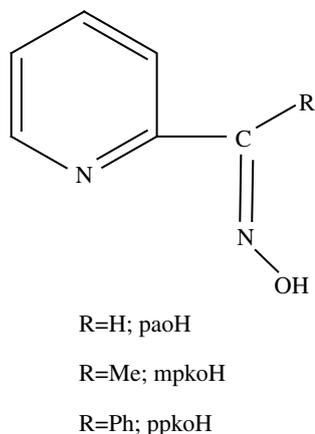
Scheme 1. The 2-pyridyl oxime ligands used in this work.

100 instrument. Magnetic susceptibility measurements were performed at room temperature by the Faraday method using a Cahn-Ventron RM-2 balance standardized with HgCo(NCS)$_4$. Pascal's constants were used to estimate the diamagnetic corrections which were subtracted from the experimental susceptibilities to give the corrected molar magnetic susceptibilities. The variable-temperature magnetic susceptibility properties of complex **2** were investigated using a M600 SQUID magnetometer.

2.2. Compound preparation

2.2.1. [Co(pao)$_3$] (1)

Method A. A pink suspension of Co(O$_2$CMe)$_2$ · 4H$_2$O (0.13 g, 0.50 mmol) in MeCN (25 ml) was treated with solid paoH (0.18 g, 1.50 mmol). The resulting orange slurry was refluxed for 2.5 h, during which time the solids dissolved and the colour of the solution turned to dark red. The solution obtained was stirred at ambient temperature for a further 1 h, during which time a dark orange microcrystalline solid rapidly precipitated. The solid product was isolated by filtration, washed with cold MeCN (2 × 3 mL) and Et$_2$O (2 × 5 mL), and dried in air for 1 h. Dissolution of the solid in MeOH (20 mL) and slow evaporation of the resulting filtrate at room temperature gave dark orange crystals of **1** after 8 days. The crystals were collected by filtration, washed with cold MeOH (1 × 2 mL) and Et$_2$O (2 × 5 mL), and dried in air. Yield 60% (based on the ligand). *Anal.* Calc. for C$_{18}$H$_{15}$CoN$_6$O$_3$: C, 51.19; H, 3.59; N, 19.91%. Found: C, 51.06; H, 3.52; N, 19.88%. Selected IR data (KBr pellet, cm^{-1}): 1602s, 1484vs, 1426s, 1348s, 1298w, 1224m, 1180m, 1148m, 1022w, 890w, 806m, 764m, 676m, 580w, 452w.

Method B. Solids Co(O$_2$CMe)$_2$ · 4H$_2$O (0.13 g, 0.50 mmol) and paoH (0.18 g, 1.50 mmol) were dissolved under refluxing conditions in a solvent mixture comprising MeCN/DMF (20 ml, 1:1 v/v) to give a dark red solution. The obtained solution was allowed to stand undisturbed at room temperature for 10 days, during which time well-formed, X-ray quality dark orange crystals of **1** appeared. The crystals were collected by filtration, washed with cold MeCN (1 × 3 mL) and Et$_2$O (2 × 5 mL), and dried in air. Yield 40% (based on the ligand). The identity of the product was confirmed by elemental analyses (C, H, N) and IR spectroscopic comparison with authentic material from Method A.

2.2.2. [Co$_3$(pao)$_6$](ClO$_4$)$_2$ (2)

Method A. An orange suspension of **1** (0.42 g, 1.00 mmol) in MeCN (30 ml) was treated with solid Co(ClO$_4$)$_2$ · 6H$_2$O (0.19 g, 0.50 mmol). The resulting orange-red slurry was refluxed for 12 h, during which time the solids dissolved and the colour of the solution turned to dark red. The solution was filtered, and

the filtrate left undisturbed at room temperature to concentrate slowly by evaporation. After 5 days, dark red crystals of **2** were collected by filtration, washed with cold MeCN (2 × 2 mL) and Et$_2$O (2 × 5 mL), and dried in air. Yield 80%. *Anal.* Calc. for C$_{36}$H$_{30}$Co$_3$N$_{12}$O$_{14}$Cl$_2$: C, 39.22; H, 2.75; N, 15.25. Found: C, 39.26; H, 2.90; N, 15.28%. Selected IR data (KBr pellet, cm^{-1}): 1606s, 1564m, 1522s, 1476m, 1438m, 1350m, 1232s, 1205m, 1148vs, 1112m, 1086vs, 902m, 770m, 678m, 628m, 590m, 466m.

Method B. A pink solution of Co(ClO$_4$)$_2$ · 6H$_2$O (0.19 g, 0.50 mmol) in MeOH (20 mL) was added to a colourless solution of paoH (0.12 g, 1.00 mmol) and Me$_4$NOH · 5H$_2$O (0.18 g, 1.00 mmol) in the same solvent (10 mL). The resulting dark red solution was stirred for 20 min, filtered, and the filtrate left undisturbed at room temperature to concentrate slowly by evaporation. After 2 days, dark red crystals of **2** were collected by filtration, washed with cold MeOH (2 × 2 mL), and dried in air. Yield 50% (based on the ligand). The identity of the product was confirmed by elemental analyses (C, H, N) and IR spectroscopic comparison with authentic material from Method A.

2.2.3. [Co(ppko)$_3$] · 0.25H$_2$O (3 · 0.25H$_2$O)

A pink suspension of Co(O$_2$CMe)$_2$ · 4H$_2$O (0.13 g, 0.50 mmol) in MeCN (30 ml) was treated with solid ppkoH (0.30 g, 1.50 mmol). The resulting orange slurry was refluxed for 1.5 h, during which time the solids dissolved and the colour of the solution turned to dark red. The solution obtained was stirred at ambient temperature for a further 30 min, during which time a dark orange microcrystalline solid rapidly precipitated. The solid product was isolated by filtration, washed with cold MeCN (2 × 3 mL) and Et$_2$O (2 × 5 mL), and dried in air for 1 h. Dissolution of the solid in DMF (15 mL) and slow evaporation of the resulting filtrate at room temperature gave dark orange crystals of **3** · 0.25H$_2$O after 12 days. The crystals were collected by filtration, washed with cold DMF (1 × 2 mL) and Et$_2$O (2 × 5 mL), and dried under vacuum. Yield 40% (based on the ligand). The dried sample analyzed as solvent-free (**3**). *Anal.* Calc. for C$_{36}$H$_{27}$CoN$_6$O$_3$: C, 66.46; H, 4.19; N, 12.92. Found: C, 66.44; H, 4.12; N, 12.88%. Selected IR data (KBr pellet, cm^{-1}): 1598m, 1522m, 1464vs, 1438s, 1222m, 1146m, 1030w, 976w, 780m, 748m, 708s, 614m, 470m.

2.2.4. [Co$_3$(ppko)$_6$](PF$_6$)$_2$ · 6MeCN (4 · 6MeCN)

Method A. An orange suspension of **3** (0.65 g, 1.00 mmol) in MeCN (30 ml) was treated with a pink aqueous solution (5 mL) of CoCl$_2$ · 6H$_2$O (0.12 g, 0.50 mmol) and NaPF$_6$ (0.17 g, 1.00 mmol). The resulting orange-red slurry was refluxed for 5 h, during which time the solids dissolved and the colour of the solution turned to dark red. The solution was filtered, and the filtrate left undisturbed at room temperature to concentrate slowly by evaporation. After 6 days, dark red crystals of **4** · 6MeCN were collected by filtration, washed with cold MeCN (2 × 2 mL), and dried under vacuum. Yield 65%. The dried sample analyzed as solvent-free (**4**). *Anal.* Calc. for C$_{72}$H$_{54}$Co$_3$N$_{12}$O$_6$P$_2$F$_{12}$: C, 46.61; H, 2.94; N, 9.06. Found: C, 46.54; H, 2.92; N, 9.18%. Selected IR data (KBr pellet, cm^{-1}): 1598m, 1524m, 1464vs, 1438m, 1358w, 1216m, 1146m, 1030w, 977w, 842vs, 776m, 746m, 706s, 658w, 612w, 558m, 466m.

Method B. Solids Co(O$_2$CMe)$_2$ · 4H$_2$O (0.13 g, 0.50 mmol), ppkoH (0.30 g, 1.50 mmol) and NaPF$_6$ (0.17 g, 1.00 mmol) were dissolved under refluxing conditions in MeCN (30 ml) to give a dark red solution. The obtained solution was stirred for a further 15 min, filtered, and the filtrate was layered with Et$_2$O (60 mL). After 4 days, dark red crystals of **4** · 6MeCN were collected by filtration, washed with cold MeCN (2 × 2 mL) and Et$_2$O (2 × 5 mL), and dried under vacuum. Yield 70% (based on the ligand). The identity of the product was confirmed by elemental analyses (C, H, N) and IR spectroscopic comparison with authentic material from Method A.

Method C. A pink solution of $CoCl_2 \cdot 6H_2O$ (0.12 g, 0.50 mmol) and $NaPF_6$ (0.17 g, 1.00 mmol) in MeOH (10 mL) was added to a pale yellow solution of ppkoH (0.20 g, 1.00 mmol) and Me_4-$NOH \cdot 5H_2O$ (0.18 g, 1.00 mmol) in MeCN (20 mL). The resulting dark red solution was stirred for 30 min, filtered, and the filtrate left undisturbed at room temperature to concentrate slowly by evaporation. After 3 days, dark red crystals of **4** · 6MeCN were collected by filtration, washed with cold MeCN (2 × 2 mL), and dried under vacuum. Yield 55% (based on the ligand). The identity of the product was confirmed by elemental analyses (C, H, N) and IR spectroscopic comparison with authentic material from Method A.

2.2.5. [Co(mpko)$_3$] · 3MeNO$_2$ (5 · 3MeNO$_2$)

Method A. A pink suspension of $Co(O_2CMe)_2 \cdot 4H_2O$ (0.13 g, 0.50 mmol) in $MeNO_2$ (30 ml) was treated with solid mpkoH (0.20 g, 1.50 mmol). The resulting orange slurry was refluxed for 3 h, during which time the solids dissolved and the colour of the solution turned to dark red. The obtained solution was stirred for a further 30 min, filtered, and the filtrate was layered with a solvent mixture comprising Et_2O/n-hexane (60 mL, 1:1 v/v). After 5 days, dark orange crystals of **5** · 3MeNO$_2$ were collected by filtration, washed with cold $MeNO_2$ (1 × 3 mL) and Et_2O (2 × 5 mL), and dried under vacuum. Yield 50% (based on the ligand). The dried sample analyzed satisfactorily as **5** · 3MeNO$_2$. *Anal.* Calc. for $C_{24}H_{30}CoN_9O_9$: C, 44.51; H, 4.68; N, 19.47. Found: C, 44.42; H, 4.62; N, 19.58%. Selected IR data (KBr pellet, cm^{-1}): 3056w, 2964w, 1636w, 1600s, 1472vs, 1430s, 1302m, 1228vs, 1156m, 1118m, 1084w, 986w, 768s, 692m, 504w, 454w.

Method B. A pink solution of $CoCl_2 \cdot 6H_2O$ (0.12 g, 0.50 mmol) in MeOH (5 mL) was added to a colourless solution of mpkoH (0.20 g, 1.50 mmol) and $Me_4NOH \cdot 5H_2O$ (0.27 g, 1.50 mmol) in $MeNO_2$ (20 mL). The resulting dark red solution was stirred for 45 min, filtered, and the filtrate left undisturbed at room temperature to concentrate slowly by evaporation. After 10 days, dark orange crystals of **5** · 3MeNO$_2$ were collected by filtration, washed with cold $MeNO_2$ (1 × 3 mL) and Et_2O (2 × 5 mL), and dried under vacuum. Yield 35% (based on the ligand). The identity of the product was confirmed by elemental analyses (C, H, N) and IR spectroscopic comparison with authentic material from Method A.

2.2.6. [Co$_3$(mpko)$_6$](PF$_6$)$_2$ (6a)

An orange suspension of **5** · 3MeNO$_2$ (0.65 g, 1.00 mmol) in MeCN (30 ml) was treated with a pink aqueous solution (5 mL) of $CoCl_2 \cdot 6H_2O$ (0.12 g, 0.50 mmol) and $NaPF_6$ (0.17 g, 1.00 mmol). The resulting orange-red slurry was refluxed for 7 h, during which time the solids dissolved and the colour of the solution turned to dark red. The solution was filtered, and the filtrate left undisturbed at room temperature to concentrate slowly by evaporation. After 4 days, a dark red microcrystalline solid appeared, which was collected by filtration, washed with cold MeCN (2 × 2 mL) and Et_2O (2 × 3 mL), and dried under vacuum. Yield 55%. The dried sample analyzed as solvent-free (**6a**). *Anal.* Calc. for $C_{42}H_{44}Co_3N_{12}O_6P_2F_{12}$: C, 39.48; H, 3.32; N, 13.16. Found: C, 39.44; H, 3.42; N, 13.18%. Selected IR data (KBr pellet, cm^{-1}): 1601m, 15548w, 1495s, 1434m, 1417w, 1223w, 1088vs, 948s, 843vs, 782m, 695w, 629s, 559m, 461m.

2.2.7. [Co$_3$(mpko)$_6$](ClO$_4$)$_2$ (6b)

An orange suspension of **5** · 3MeNO$_2$ (0.65 g, 1.00 mmol) in MeCN (30 ml) was treated with solid $Co(ClO_4)_2 \cdot 6H_2O$ (0.19 g, 0.50 mmol). The resulting orange-red slurry was refluxed for 10 h, during which time the solids dissolved and the colour of the solution turned to dark red. The solution was filtered, and the filtrate left undisturbed at room temperature to concentrate slowly by evaporation. After 6 days, a dark red microcrystalline solid appeared, which was collected by filtration, washed with cold MeCN (2 × 2 mL) and Et_2O (2 × 3 mL), and dried under vacuum. Yield 60%. The dried sample analyzed as solvent-free (**6b**). *Anal.* Calc. for $C_{42}H_{44}Co_3N_{12}O_{14}Cl_2$: C, 42.50; H, 3.57; N, 14.17. Found: C, 42.54; H, 3.62; N, 14.38%. Selected IR data (KBr pellet, cm^{-1}): 1602m, 1554w, 1490s, 1438m, 1414w, 1222w, 1088vs, 948s, 782m, 696w, 624s, 460m.

2.3. Single-crystal X-ray crystallography

The crystallographic data and structure refinement details for the five, structurally characterized complexes are summarized in Table 1. Selected crystals of **1** (0.12 × 0.16 × 0.22 mm), **2** (0.15 × 0.16 × 0.20 mm), **4** · 6MeCN (0.05 × 0.10 × 0.55 mm) and **5** · 3MeNO$_2$ (0.30 × 0.40 × 0.50 mm) were mounted in capillary,

Table 1
Crystallographic data for complexes **1**, **2**, **3** · 0.25H$_2$O, **4** · 6MeCN and **5** · 3MeNO$_2$.

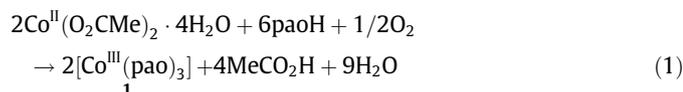| Parameter	1	2	3·0.25H$_2$O	4·6MeCN	5·3MeNO$_2$
Formula	$C_{18}H_{15}CoN_6O_3$	$C_{36}H_{30}Co_3N_{12}O_{14}Cl_2$	$C_{36}H_{27.5}N_6CoO_{3.25}$	$C_{84}H_{72}Co_3N_{18}O_6P_2F_{12}$	$C_{24}H_{30}CoN_9O_9$
Formula weight	422.29	1102.44	655.07	1896.32	647.50
Crystal system	orthorhombic	hexagonal	monoclinic	triclinic	hexagonal
Space group	$Pbca$	$R\bar{3}$	$P2_1/c$	$P\bar{1}$	$R\bar{3}$
α (Å)	15.8383(8)	14.213(5)	9.980(10)	13.909(8)	15.415(6)
b (Å)	12.5001(7)	14.213(5)	10.810(10)	15.61(1)	15.415(6)
c (Å)	17.2242(8)	19.992(8)	27.98(3)	10.793(7)	21.249(8)
α (°)	90	90	90	89.98(2)	90
β (°)	90	90	94.98(4)	82.71(2)	90
γ (°)	90	120	90	73.31(2)	120
V (Å^3)	3410.1(3)	3497(2)	3007(5)	2225(2)	4373(3)
Z	8	3	4	1	6
ρ_{calc} (g cm^{-3})	1.645	1.570	1.447	1.415	1.475
Radiation, λ (Å)	Mo Kα, 0.71073	Mo Kα, 0.71073	Mo Kα, 0.71073	Mo Kα, 0.71073	Mo Kα, 0.71073
Temperature (K)	100	298	298	298	298
μ (mm^{-1})	1.042	1.245	0.620	0.675	0.655
Data collected/unique	33131/5658	2906/1368	3086/3009	8284/7832	3645/1723
(R_{int})	(0.0641)	(0.0274)	(0.0291)	(0.0155)	(0.0259)
Data with $I > 2\sigma(I)$	3896	1214	2283	5537	1559
R_1 ($I > 2\sigma(I)$)[a]	0.0439	0.0353	0.0529	0.0620	0.0425
wR_2 ($I > 2\sigma(I)$)[b]	0.1303	0.0957	0.1311	0.1650	0.1164

[a] $R_1 = \Sigma(|F_o| - |F_c|)/\Sigma(|F_o|)$.
[b] $wR_2 = \sum[w(F_o^2 - F_c^2)^2]/\sum[w(F_o^2)^2]^1/2$.

whereas a selected crystal of $3 \cdot 0.25H_2O$ (0.08 × 0.15 × 0.40 mm) was mounted in air. Diffraction measurements were made on a Crystal Logic Dual Goniometer diffractometer using graphite-monochromated Mo radiation. Unit cell dimensions were determined and refined by using the angular settings of 25 automatically centered reflections in the range $11 < 2\theta < 23°$. Intensity data were recorded using a $\theta - 2\theta$ scan to a maximum 2θ value of 50°. Three standard reflections monitored every 97 reflections showed less than 3% variation and no decay. Lorentz, polarization corrections were applied using Crystal Logic software. All five structures were solved by direct methods using SHELXS-86 [11a] and refined on F^2 by full-matrix least squares techniques with SHEL-XL-97 [11b]. All H atoms were located by Fourier difference maps and refined isotropically, except those on the solvent molecules ($3 \cdot 0.25H_2O$, $4 \cdot 6MeCN$ and $5 \cdot 3MeNO_2$) which were introduced at calculated positions as riding on bonded atoms. All non-H atoms were refined anisotropically.
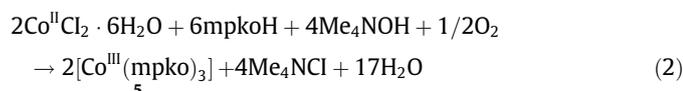
3. Results and discussion
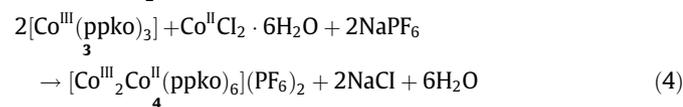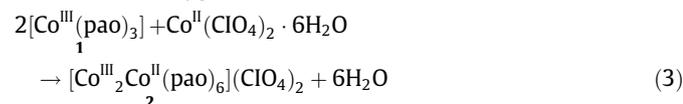
3.1. Brief synthetic comments and IR spectra

Aerobic reactions of $Co(O_2CMe)_2 \cdot 4H_2O$ with the appropriate 2-pyridyl oximes in an 1:3 ratio in various solvents under reflux gave dark red solutions, from which were subsequently isolated the orange mononuclear Co^{III} complexes **1**, **3** and **5**, upon conventional workup. The formation of the representative compound **1** can be represented by Eq. (1)

$$2Co^{II}(O_2CMe)_2 \cdot 4H_2O + 6paoH + 1/2O_2$$
$$\rightarrow 2[\underset{\mathbf{1}}{Co^{III}(pao)_3}] + 4MeCO_2H + 9H_2O \qquad (1)$$

The $MeCO_2^-$ ions act as a base deprotonating the two-thirds (2/3) of the amount of the organic ligand. Note that **1** and **3** have the *trans* (or *mer*) configuration, whereas complex **5** is the *cis* (or *fac*) isomer (vide infra). The three complexes can be also prepared by the 1:3 aerobic reactions between $CoCl_2 \cdot 6H_2O$ and the oximes in various solvents *in the presence of a base*, see Eq. (2). A typical such preparation is reported in Section 2.2.5 (Method B)

$$2Co^{II}Cl_2 \cdot 6H_2O + 6mpkoH + 4Me_4NOH + 1/2O_2$$
$$\rightarrow 2[\underset{\mathbf{5}}{Co^{III}(mpko)_3}] + 4Me_4NCl + 17H_2O \qquad (2)$$
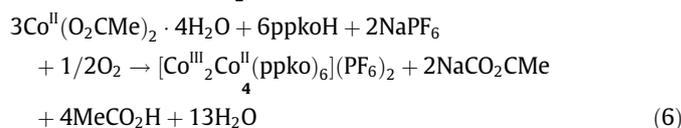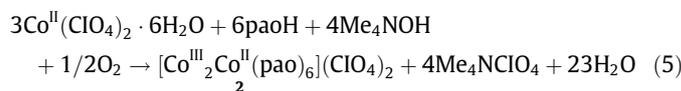
Since **1**, **3** and **5** each possesses three free, i.e. uncoordinated, oxime oxygen atoms, we suspected that these mononuclear Co^{III} complexes could act as "ligands" (the so-named "metal complexes as ligands strategy" [5]) and would further react with Co^{II} sources leading to mixed-valent Co^{II}/Co^{III} clusters; such clusters are of great current magnetochemical interest [12]. This, indeed, turned out to be the case and led to the trinuclear $Co_2^{III}Co^{II}$ clusters **2**, **4**, **6a** and **6b**; typical preparations are illustrated by Eqs. (3) and (4). The three oxime oxygen atoms that had been free in the

$$2[\underset{\mathbf{1}}{Co^{III}(pao)_3}] + Co^{II}(ClO_4)_2 \cdot 6H_2O$$
$$\rightarrow [\underset{\mathbf{2}}{Co^{III}_2Co^{II}(pao)_6}](ClO_4)_2 + 6H_2O \qquad (3)$$

$$2[\underset{\mathbf{3}}{Co^{III}(ppko)_3}] + Co^{II}Cl_2 \cdot 6H_2O + 2NaPF_6$$
$$\rightarrow [\underset{\mathbf{4}}{Co^{III}_2Co^{II}(ppko)_6}](PF_6)_2 + 2NaCl + 6H_2O \qquad (4)$$

mononuclear precursors **1**, **3** and **5** were indeed coordinated to the Co^{II} center in **2**, **4**, **6a** and **6b**. Two Co centers are in the oxidation state III and the products are thus cationic. Therefore, an appropriate counteranion should be present in the reaction mixture, either as the inorganic anion of the Co^{II} source (ClO_4^-) or added externally

(PF_6^-). The trinuclear clusters have the three oximate groups of each corresponding Co^{III} metalloligand in a *fac* configuration around the Co^{II} center (vide infra). Since the oximate disposition is different in **1**, **3** and **5** (*mer* versus *fac*), we anticipated different products from the reactions of the metalloligands **1** and **3** with the Co^{II} source compared with the product from the reaction of **5** with Co^{II}. In a sense, complexes **1** and **3** can be considered as bidentate-monodentate bridging "ligands" (due to the *mer* geometry of the three, free oximate oxygens), whereas complex **5** can be viewed as a tridentate chelating "ligand" (due to the *fac* geometry of the three, free oximate oxygens). Somewhat to our surprise, however, the molecular structures of the trinuclear cations seem to be very similar. This means that the geometry of **5** only is preserved in the trinuclear cluster cation (**6a** and **6b**). The *mer* isomers **1** and **3** are also converted to mixed-valent, trinuclear cations (**2** and **4**) that contain the *fac*-$[Co^{III}(pao)_3]$ and *fac*-$[Co^{III}(ppko)_3]$ metalloligand units, respectively. This may suggest the occurrence of an equilibrium between *mer* and *fac* mononuclear, 1:3 Co^{III} species in solution (at least for **1** and **3**), which shifts to the *fac* isomer upon addition of external Co^{II}.

Complexes **2**, **4**, **6a** and **6b** can be also prepared under aerobic conditions by "one-pot" procedures involving the appropriate reaction mixture of a Co^{II} starting material, counteranion and 2-pyridyl oxime, in the presence (when the inorganic anions present are ClO_4^-, Cl^-/ClO_4^- or Cl^-/PF_6^-) or absence (when $MeCO_2^-$ ions are present) of external OH^- ions. Typical preparations are reported in Sections 2.2.2 (Method B) and 2.2.4 (Methods B and C) and illustrated by Eqs. (5) and (6)

$$3Co^{II}(ClO_4)_2 \cdot 6H_2O + 6paoH + 4Me_4NOH$$
$$+ 1/2O_2 \rightarrow [\underset{\mathbf{2}}{Co^{III}_2Co^{II}(pao)_6}](ClO_4)_2 + 4Me_4NClO_4 + 23H_2O \qquad (5)$$

$$3Co^{II}(O_2CMe)_2 \cdot 4H_2O + 6ppkoH + 2NaPF_6$$
$$+ 1/2O_2 \rightarrow [\underset{\mathbf{4}}{Co^{III}_2Co^{II}(ppko)_6}](PF_6)_2 + 2NaCO_2CMe$$
$$+ 4MeCO_2H + 13H_2O \qquad (6)$$

The IR spectra of complexes **2** and **6a** exhibit bands near 1090 and 625 cm^{-1}, due to the $\nu_3(F_2)[\nu_d(ClO)]$ and $\nu_4(F_2)[\delta_d(OClO)]$ modes of the uncoordinated T_d ClO_4^- ions, respectively [13]. A strong band at ~840 cm^{-1} and a medium-intensity band at ~560 cm^{-1} in the spectra of **4** and **6b** are assigned [13] to the $\nu_3(F_{1u})[\nu(PF)]$ and $\nu_4(F_{1u})[\delta(FPF)]$ vibrations of the O_h PF_6^- ion, confirming its ionic nature. Two bands, one of variable intensity at 1228–1205 cm^{-1} assigned to $\nu(N-O)$ and one of medium to strong intensity at 1606–1598 cm^{-1} assigned to $\nu(C=N)_{oximate}$, are common in the spectra of all the prepared complexes [14]; the higher-wavenumber band most probably overlaps with a 2-pyridyl stretch. The $\nu(N-O)$ band is located at a slightly lower wavenumber in **2**, **4**, **6a** and **6b** than for their corresponding metalloligand Co^{III} complexes **1**, **3** and **5**, respectively, consistent with the oximate O-coordination in the trinuclear clusters. The in-plane deformation bands of the 2-pyridyl ring of the free paoH, ppkoH and mpkoH ligands at 620–650 cm^{-1} shift upwards (708–676 cm^{-1}) in the spectra of the mononuclear and trinuclear compounds, confirming the involvement of the ring-N atom in coordination [15]. The similar spectral behaviour of **6a** and **6b** (we could not grow single crystals of these complexes suitable for their X-ray structural characterization) in the regions of the $\nu(C=N)_{oximate}$, $\nu(N-O)$ and $\delta(Py)$ vibrations, compared with that of the structurally characterized trinuclear complexes **2** and **4**, is a strong evidence that the cations of the former are structurally analogous to the cations of **2** and **4**.

3.2. Description of structures

The molecular structures of the mononuclear complexes **1**, **3** and **5** are depicted in Figs. 1–3, respectively. Selected interatomic
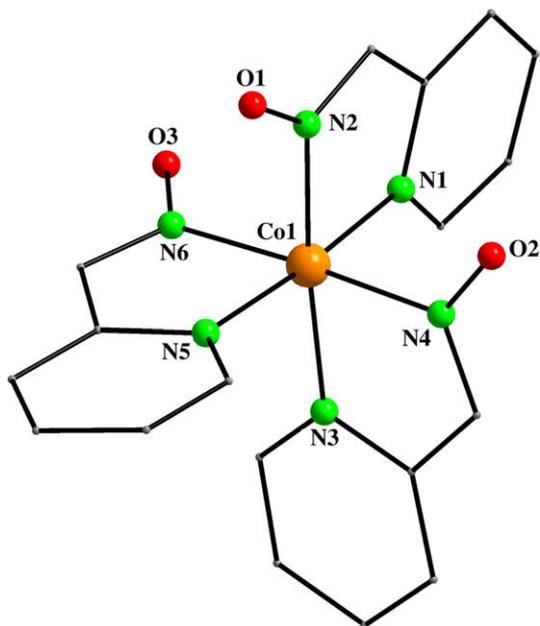
Fig. 1. Molecular structure of complex **1** with selected atom labelling. H atoms have been omitted for clarity. Colour scheme: Co^{III}, orange; O, red; N, green; C, gray.
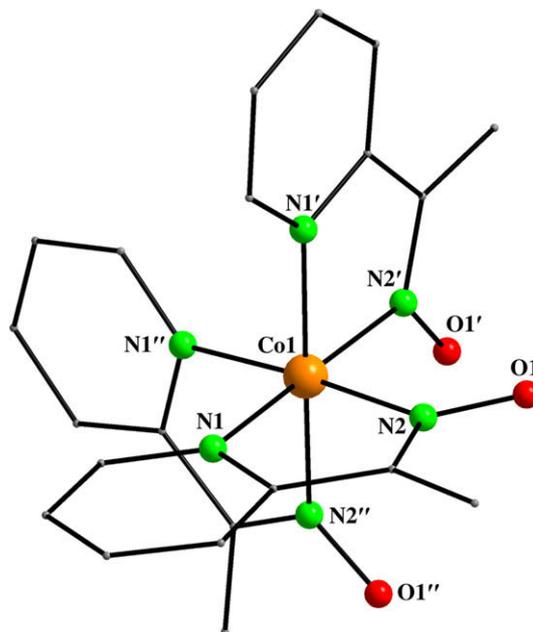

Fig. 2. Partially labelled plot of complex **3**; colour scheme as in Fig. 1. H atoms have been omitted for clarity.
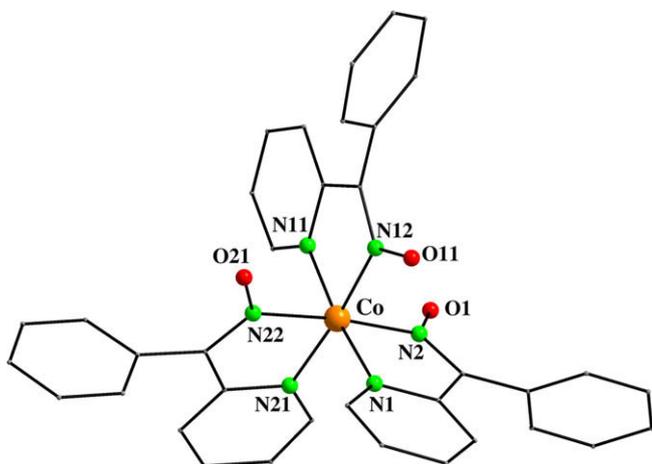

Fig. 3. Partially labelled plot of complex **5**; colour scheme as in Fig. 1. H atoms have been omitted for clarity.

Table 2
Selected bond lengths (Å) and angles (°) for complexes **1**, **3**·0.25H$_2$O and **5**·3MeNO$_2$.

Parameter[a]		Parameter	
1			
Co(1)–N(1)	1.921(2)	N(1)–Co(1)–N(3)	94.2(7)
Co(1)–N(2)	1.909(2)	N(1)–Co(1)–N(5)	175.3(7)
Co(1)–N(3)	1.958(2)	N(2)–Co(1)–N(3)	174.6(7)
Co(1)–N(4)	1.943(2)	N(2)–Co(1)–N(4)	92.4(7)
Co(1)–N(5)	1.931(2)	N(2)–Co(1)–N(6)	90.0(7)
Co(1)–N(6)	1.941(2)	N(3)–Co(1)–N(5)	88.7(7)
		N(4)–Co(1)–N(6)	176.5(7)
3 · 0.25H$_2$O			
Co–N(1)	1.927(5)	N(1)–Co–N(11)	172.7(2)
Co–N(2)	1.920(5)	N(1)–Co–N(21)	93.6(2)
Co–N(11)	1.931(5)	N(2)–Co–N(12)	92.2(2)
Co–N(12)	1.907(5)	N(2)–Co–N(22)	174.0(2)
Co–N(21)	1.949(5)	N(11)–Co–N(21)	93.6(2)
Co–N(22)	1.934(5)	N(12)–Co–N(21)	174.3(2)
		N(12)–Co–N(22)	92.7(2)
5 · 3MeNO$_2$			
Co(1)–N(1)	1.946(2)	N(1)–Co(1)–N(2')	176.1(8)
Co(1)–N(1')	1.946(2)	N(1')–Co(1)–N(2'')	176.1(8)
Co(1)–N(1'')	1.946(2)	N(1'')–Co(1)–N(2)	176.1(8)
Co(1)–N(2)	1.905(2)	N(1)–Co(1)–N(1')	95.2(9)
Co(1)–N(2')	1.905(2)	N(2)–Co(1)–N(2')	93.9(9)
Co(1)–N(2'')	1.905(2)		

[a] Unprimed, primed and doubly-primed atoms have the symmetry operators (−1 + x − y, 1 − y, z), (x, y, z) and (1 − x, 2 − x + y, z), respectively.

distances and angles for the same compounds are listed in Table 2. Partially labelled representations of the cations of complexes **2** and **4** are shown in Figs. 4 and 5, respectively, while their selected interatomic distances and angles are listed in Table 3.

Complex **1** crystallizes in the orthorhombic space group *Pbca*. Its structure consists of well-separated [Co(pao)$_3$] molecules. The Co^{III} ion is coordinated by three N,N′-bidentate chelating (or 1.011 [16]) pao⁻ ligands. The pao⁻ donor atoms are the nitrogen atoms of the deprotonated oxime and the 2-pyridyl groups. The six-coordinate molecule is the *mer* (or *trans*) isomer. Complex **3** · 0.25H$_2$O crystallizes in the monoclinic space group *P*2$_1$/c and its structure comprises mononuclear [Co(ppko)$_3$] units and solvate H$_2$O molecules; the latter will not be further discussed. The six-coordinate Co^{III} ion possesses a distorted octahedral geometry and is (similarly to **1**) the *mer* isomer. The coordination sphere of the Co^{III} atom in **3** · 0.25H$_2$O consists of three N,N′-bidentate chelating (or 1.011 [16]) ppko⁻ ligands. The molecular structures of **1** and **3** are very similar, and the replacement of the H atom by the

Ph group has thus little structural effect. Complex **5** · 3MeNO$_2$ crystallizes in the hexagonal space group *R*$\bar{3}$, with mononuclear [Co(mpko)$_3$] units and solvate MeNO$_2$ molecules in general positions. The Co^{III} ion, which sits on a 3-fold axis of symmetry, is coordinated by three N,N′-bidentate chelating (or 1.011 [16]) mpko⁻ ligands. Surprisingly, and by contrast with **1** and **3**, the six-coordinate complex **5** · 3MeNO$_2$ is the *fac* (or *cis*) isomer. The Co-N bond lengths agree well with values expected for low-spin Co^{III} in octahedral environments [4]. The observed, similar coordination modes of the oximate ligands in complexes **1**, **3** and **5** are interesting because the deprotonated oxygen atom remains uncoordinated.
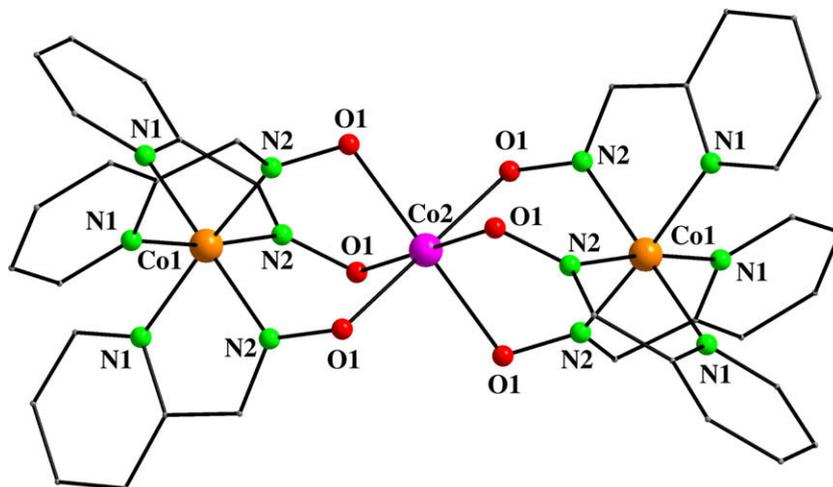
Fig. 4. Partially labelled representation of the mixed-valence(III/II/III) cation [Co$_3$(pao)$_6$]$^{2+}$ present in complex **2**. Identical numbers are used for atoms generated by symmetry. H atoms have been omitted for clarity. Colour scheme: Co^{II}, pink; Co^{III}, orange; O, red; N, green; C, gray.
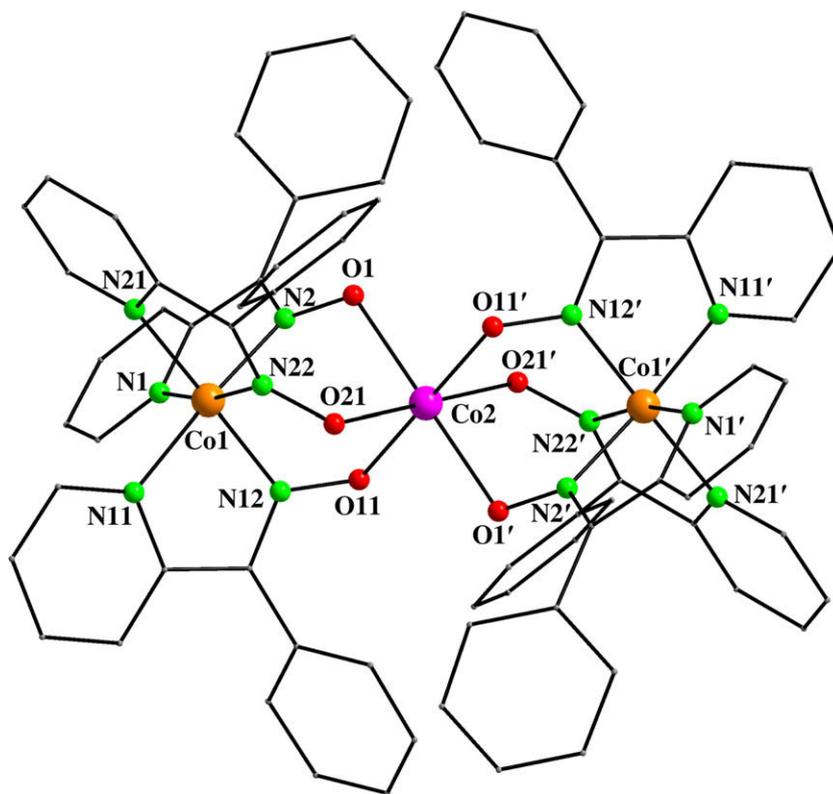

Fig. 5. Molecular structure of the mixed-valence (III/II/III) cation [Co$_3$(ppko)$_6$]$^{2+}$ present in complex **4**·6MeCN with selected atom labelling; colour scheme as in Fig. 4. Primes are used for symmetry-related ($-x, -y, -z$) atoms. H atoms have been omitted for clarity.

The cations of **2** (Fig. 4) and **4** (Fig. 5) are structurally similar in many aspects, except the nature of the coordinated 2-pyridyl oximate group (pao$^-$ versus ppko$^-$) and the counteranion (ClO$_4^-$ versus PF$_6^-$), and thus only the structure of complex **2** will be described in detail. The crystal structure of **2** reveals the formation of a linear trinuclear cation. The central metal ion, Co(2), sits on a 3-fold inverse axis of symmetry, while the terminal metal ion, Co(1), sits on a 3-fold symmetry axis. The central metal ion is octahedrally coordinated by six oxygen atoms [O(1), and its symmetry-related partners] belonging to six pao$^-$ ligands. The six coordina-

tion sites on each of the distorted octahedral, terminal Co ions are occupied by the nitrogen atoms [N(1), N(2), and their symmetry-related partners] that belong to the "chelating" part of three pao$^-$ ligands, with the three oximate N atoms in the facial (or *cis*) configuration. The core for **2** (and **4**) appears to be [Co^{II}Co$_2^{III}$(µ-ONR')$_6$]$^{2+}$. Charge considerations require a formal 2Co^{III},Co^{II} description of **2** (and **4**), and the terminal metal ions are clearly low-spin Co^{III} ions based on their Co–N bond lengths (all <1.96 Å), which have lengths similar to Co^{III}–N bond lengths in other structurally characterized cobalt(III) complexes with

Table 3
Selected bond lengths (Å) and angles (°) for complexes **2** and **4**·6MeCN.

Parameter[a]		Parameter	
2			
Co(1)–N(1)	1.961(2)	N(1)–Co(1)–N(1)	93.6(8)
Co(1)–N(2)	1.899(2)	N(1)–Co(1)–N(2)	172.0(8)
Co(2)–O(1)	2.102(2)	N(2)–Co(1)–N(2)	91.2(7)
		O(1)–Co(2)–O(1)	180.0(9)
4·6MeCN			
Co(1)–N(1)	1.945(4)	Co(2)–O(1)	2.127(3)
Co(1)–N(2)	1.901(4)	Co(2)–O(1′)	2.127(3)
Co(1)–N(11)	1.955(4)	Co(2)–O(11)	2.077(3)
Co(1)–N(12)	1.881(4)	Co(2)–O(11′)	2.077(3)
Co(1)–N(21)	1.955(4)	Co(2)–O(21)	2.110(3)
Co(1)–N(22)	1.905(4)	Co(2)–O(21′)	2.110(3)
N(1)–Co(1)–N(22)	169.1(2)	N(2)–Co(1)–N(22)	88.4(2)
N(2)–Co(1)–N(11)	173.8(2)	N(12)–Co(1)–N(22)	92.0(2)
N(12)–Co(1)–N(21)	173.8(2)	O(1)–Co(2)–O(1′)	180.0(3)
N(1)–Co(1)–N(11)	94.8(2)	O(11)–Co(2)–O(11′)	180.0(3)
N(1)–Co(1)–N(21)	92.1(2)	O(21)–Co(2)–O(21′)	180.0(3)
N(11)–Co(1)–N(21)	94.7(2)	O(1)–Co(2)–O(11)	90.6(1)
N(2)–Co(1)–N(12)	92.5(2)	O(1)–Co(2)–O(21)	87.3(1)
		O(11)–Co(2)–O(21)	91.2(1)

[a] Primes are used for symmetry-related ($-x, -y, -z$) atoms.

N-ligation [4]. The central cobalt center [Co(2)] has all six Co–O distances 2.102(2) Å indicating that this is a Co^{II} ion [4]. The pao⁻ ions in **2** (and the ppko⁻ groups in **4**) function as $\eta^1:\eta^1:\eta^1:\mu$ ligands (or as $2.1_11_21_2$ ligands using Harris notation [16]); each ligand chelates one Co^{III} ion through the 2-pyridyl and the oximate nitrogen atoms forming a five-membered chelating ring, and bridges this metal center with the central Co^{II} ion through the terminally ligated, deprotonated oxygen atom. Complexes **2** and **4** join a handful of structurally characterized linear, valence-trapped $Co^{III}Co^{II}Co^{III}$ clusters [17].

3.3. Magnetochemistry and ligand-field spectra

Complexes **1**, **3**·0.25H₂O and **5**·3MeNO₂ are diamagnetic, as expected. The room-temperature, effective magnetic moment (μ_{eff}) values of **2**, **4**, **6a** and **6b** are 4.81, 5.13, 4.99 and 5.07 B.M. per trimer, respectively; these values are consistent with the presence of one high-spin Co^{II} ion with octahedral stereochemistry [18].

The μ_{eff} value of the representative trinuclear cluster **2** decreases gradually to 4.01 B.M. per trimer at 25 K and then drops to 3.53 B.M. at 2.0 K. This behaviour may be understood as arising from the combined effects of orbital degeneracy and zero-field splitting [17h].

The solid-state (diffuse reflectance) UV–Vis spectra of **1**, **3**·0.25H₂O and **5**·3MeNO₂ are typical for low-spin $Co^{III}N_6$ chromophores [19]. The low-spin octahedral ground term is $^1A_{1g}$ and there are two relatively low lying spin allowed transitions, with lower lying spin triplet partners, all derived from $(t_{2g})^5(e_g)$. Under this scheme, the bands in the spectrum of **5**, for example, at 29.13, 21.35, 17.10 and 13.36 kK are assigned [19] to the $^1A_{1g} \rightarrow {}^1T_{2g}, {}^1T_{1g}, {}^3T_{2g}$ and $^3T_{1g}$ transitions, respectively. The spectra of the trinuclear $Co^{III}Co^{II}Co^{III}$ clusters exhibit bands at approximately the same energies with those of their corresponding mononuclear Co^{III} complexes, and maxima characteristic of octahedral $Co^{II}O_6$ chromophores [19]. For instance, the spectrum of **6a** shows bands/shoulders at 29.27, 21.55, 17.50 and 13.00 kK due to its fac-[Co^{III}(mpko)₃] units (and assigned as above), and additional bands at 19.23 and 15.80 kK due to its high-spin octahedral $Co^{II}(O_{oximato})_6$ unit and assigned (under O_h symmetry) to the $^4T_{1g} \rightarrow {}^4T_{1g}(P), {}^4A_{2g}$ transitions, respectively [19]. The electronic spectra of **2**, **4** and **6b** are very similar supporting similar structures.

4. Conclusions

This work extends the body of results that emphasize the ability of the anionic 2-pyridyl oximate ligands to form interesting structural types in 3d-metal chemistry. The initial use of pao⁻, ppko⁻ and mpko⁻ in Co non-carboxylate chemistry has provided access to diamagnetic mononuclear Co^{III} complexes and to paramagnetic mixed-valence $Co_2^{III}Co^{II}$ clusters. The incorporation of only one Co^{II} center in the trinuclear clusters precludes the observation of interesting magnetic properties as these complexes behave as mononuclear Co^{II} species. The flexibility of the 2-pyridyl oximate ligands and some very recent results in our group let us believe that we have only seen the tip of the iceberg in Co/2-pyridyl oximate chemistry and that some new clusters with interesting magnetic properties await discovery. From the synthetic inorganic chemistry viewpoint, this work demonstrates the utility of the "metal complexes as ligands" approach in transition metal cluster chemistry. Preliminary experiments show that the reactions of **1–3** with sources of other divalent 3d metals lead to a variety of mixed-metal Co^{III}/M^{II} complexes (M = Fe, Mn, Ni, Cu).

5. Supplementary data

CCDC 264168, 264167, 264166, 264165 and 264169 contains the supplementary crystallographic data for **1**, **2**, (**3**·0.25H₂O), (**4**·6MeCN), and (**5**·3MeNO₂). These data can be obtained free of charge via http://www.ccdc.cam.ac.uk/conts/retrieving.html, or from the Cambridge Crystallographic Data Centre, 12 Union Road, Cambridge CB2 1EZ, UK; fax: (+44) 1223-336-033; or e-mail: deposit@ccdc.cam.ac.uk.

References

[1] R.E.P. Winpenny, in: J.P. Sauvage (Ed.), Transition Metals in Supramolecular Chemistry, vol. 5, Wiley, Chichester, 1999, pp. 193–223.
[2] (a) For reviews, see: G. Christou, D. Gatteschi, D.N. Hendrickson, R. Sessoli, MRS Bull. 25 (2000) 66;
(b) D. Gatteschi, R. Sessoli, Angew. Chem., Int. Ed. 42 (2003) 268;
(c) R. Birchner, G. Chaboussant, C. Dobe, H.U. Güdel, S.T. Ochsenbein, A. Sieber, O. Waldman, Adv. Funct. Mater. 16 (2006) 209;
(d) G. Aromi, E.K. Brechin, Struct. Bonding 122 (2006) 1.
[3] (a) E.-C. Yang, D.N. Hendrickson, W. Wernsdorfer, M. Nakano, L.N. Zakharov, R.D. Sommer, A.L. Rheingold, M. Ledezma-Gairraud, G. Christou, J. Appl. Phys. 91 (2002) 7382;
(b) M. Murrie, S.J. Teat, H. Stoeckli-Evans, H.U. Güdel, Angew. Chem., Int. Ed. 42 (2003) 4653;
(c) S.J. Langley, M. Helliwell, R. Sessoli, P. Rosa, W. Wernsdorfer, R.E.P. Winpenny, Chem. Commun. (2005) 5029;
(d) A.K. Boudalis, C.P. Raptopoulou, B. Abarca, R. Ballesteros, M. Chadlaoui, J.-P. Tuchagues, A. Terzis, Angew. Chem., Int. Ed 45 (2006) 432;
(e) Y.-Z. Zhang, W. Wernsdorfer, F. Pan, Z.-H. Wang, S. Gao, Chem. Commun. (2006) 3302;
(f) M.-H. Zeng, M.-X. Yao, H. Liang, W.-X. Zhang, M.-X. Chen, Angew. Chem., Int. Ed. 46 (2007) 1832;
(g) A. Ferguson, A. Parkin, J. Sanchez-Benitez, K. Kamenev, W. Wernsdorfer, M. Murrie, Chem. Commun. (2007) 3473.
[4] (a) For example, see: Th.C. Stamatatos, A.K. Boudalis, K.V. Pringouri, C.P. Raptopoulou, A. Terzis, J. Wolowska, E.J.L. McInnes, S.P. Perlepes, Eur. J. Inorg. Chem. (2007) 5098;
(b) Th.C. Stamatatos, S. Dionyssopoulou, G. Efthymiou, P. Kyritsis, C.P. Raptopoulou, A. Terzis, R. Vicente, A. Escuer, S.P. Perlepes, Inorg. Chem. 44 (2005) 3374.
[5] G. Denti, S. Serroni, S. Campagna, A. Juris, M. Ciano, V. Balzani, in: A.F. Williams, C. Floriani, A.E. Merbach (Eds.), Perspectives in Coordination Chemistry, VCH, Weinheim, 1992, pp. 153–164.

[6] For a comprehensive review, see: C.J. Milios, Th.C. Stamatatos, S.P. Perlepes, Polyhedron 25 (2006) 134 (Polyhedron Report).

[7] For example, see: Th.C. Stamatatos, D. Foguet-Albiol, S.-C. Lee, C.C. Stoumpos, C.P. Raptopoulou, A. Terzis, W. Wernsdorfer, S.O. Hill, S.P. Perlepes, G. Christou, J. Am. Chem. Soc. 129 (2007) 9484.

[8] For example, see: H. Miyasaka, R. Clérac, K. Mizushima, K. Sugiura, M. Yamashita, W. Wernsdorfer, C. Coulon, Inorg. Chem. 42 (2003) 8203.

[9] Th.C. Stamatatos, A. Bell, P. Cooper, A. Terzis, C.P. Raptopoulou, S.L. Heath, R.E.P. Winpenny, S.P. Perlepes, Inorg. Chem. Commun. 8 (2005) 533.

[10] M. Orama, H. Saarinen, J. Korvenranta, J. Coord. Chem. 22 (1990) 183.

[11] (a) G.M. Sheldrick, SHELXS-86, Structure Solving Program, University of Göttingen, Germany, 1986;
(b) G.M. Sheldrick, SHELXS-97, Program for the Refinement of Crystal Structures from Diffraction Data, University of Göttingén, Germany, 1997.

[12] For Example, see: L.F. Chibotaur, L. Ungur, C. Aronica, H. Elmoll, G. Pilet, D. Luneau, J. Am. Chem. Soc. 130 (2008) 12445.

[13] K. Nakamoto, Infrared and Raman Spectra of Inorganic and Coordination Compounds, 4th ed., Wiley, New York, 1986. pp. 147–155, 251.

[14] D. Burdinski, F. Birkelbach, T. Weyhermüller, U. Flörke, H.-J. Haupt, M. Lengen, A.X. Trautwein, E. Bill, K. Wieghardt, P. Chaudhuri, Inorg. Chem. 37 (1998) 1009.

[15] C. Papatriantafyllopoulou, C.G. Efthymiou, C.P. Raptopoulou, A. Terzis, E. Manessi-Zoupa, S.P. Perlepes, Spectrochim. Acta Part A 70 (2008) 718.

[16] R.A. Coxall, S.G. Harris, D.K. Henderson, S. Parsons, P.A. Tasker, R.E.P. Winpenny, J. Chem. Soc., Dalton Trans. (2000) 2349.

[17] (a) For example, see: J.A. Bertrand, J.A. Kelley, E.G. Vassian, J. Am. Chem. Soc. 91 (1969) 2394;
(b) D.A. House, V. McKee, P.J. Steel, Inorg. Chem. 25 (1986) 4884;
(c) V.M. Novorortsev, O.G. Ellert, T.S. Kapanadze, A.Y. Buslaev, Koord. Khim. 14 (1986) 856;
(d) C. Fukuhara, E. Asato, T. Shimoji, K. Katsura, M. Mori, K. Matsumoto, S. Ooi, J. Chem. Soc., Dalton Trans. (1987) 1305;
(e) B. Ballet, A. Bino, S. Cohen, H. Rubin, T. Zor, Inorg. Chim. Acta 188 (1991) 91;
(f) A. Golobic, B. Stefane, S. Polance, Polyhedron 18 (1999) 3661;
(g) T.S. Billson, J.D. Crane, O.D. Fox, S.L. Heath, Inorg. Chem. Commun. 3 (2000) 718;
(h) M. Rat, R.A. de Sousa, A. Tomas, Y. Frapart, J.-P. Tuchagues, I. Artaud, Eur. J. Inorg. Chem. (2003) 759;
(i) S. Pal, A.K. Barik, S. Gupta, S. Roy, T.N. Mandal, A. Hazra, M.S. El Fallah, R.J. Butcher, S.-M. Peng, G.-H. Lee, S.K. Kar, Polyhedron 27 (2008) 357.

[18] F.A. Cotton, G. Wilkinson, C.A. Murillo, M. Bochmann, Advanced Inorganic Chemistry, 6th ed., Wiley, New York, 1999. pp. 820–824.

[19] A.B.P. Lever, Inorganic Electronic Spectroscopy, 2nd ed., Elsevier, Amsterdam, 1984. pp. 463, 464, 473–478, 480–489.